ME105 Lab 2: Heat Transfer

Vedad Bassari, Michael Howo, and Connor Tang

December 15, 2022

1 Problem Statement

The objective of this lab is to examine heat transfer phenomenon using temperature sensors. In specific, the experiments focus on characterizing convective and conductive cooling/heating using a thermocouple, a resistance temperature detector (RTD), and a thermistor. The analysis will span the characterization of both the measurement systems and thermal responses.

The first week of the lab is allocated to calibrating the sensors and modeling their dynamic response as first-order systems, as well as an exercise regarding conservation of energy. The second week examines natural and forced convective cooling with air and water using the equipment characterized in week one and fluid mechanics theory.

2 Method

Before calibrating the temperature sensors, the thermometer needed to be validated in order to give a precise reference point. This validation would be used to calibrate the sensors later on in the lab. This was done by dipping the thermometer into an ice bath and boiling water, with e 0°C and 100°C respectively. The thermometer works by having a bulb filled with a substance that expands when the temperature of the thermometer increases and contracts when the temperature decreases.

After validating the thermometer, the calibration of the temperature sensors to map their outputs to a temperature was next. Calibration was done by dipping the sensors in varying temperatures of water and waiting for their steady state response. The temperature of the water is recorded using the thermometer that was validated earlier. Both the response output and the temperature were recorded, and the data is presented later in this report (section 4). Three temperature sensors were calibrated: a thermocouple, an RTD, and thermistor. The thermocouple works by taking two different metals (in this lab, chromium and aluminium were used) and measuring the voltage gradient it creates when introduced to a temperature gradient. This change is known as the thermoelectric effect, and it is due to electrons in the metal moving diffusing from the hot side of the thermocouple to the cold side, creating this voltage difference. This voltage difference is recorded using a LabVIEW VI, along with the time it took to reach the steady state. The RTD is similar to the thermocouple, but rather than measuring the voltage change, it measures the change in the metal's resistance. As the temperature of the RTD's metal increases, the resistance increases as well due to the higher temperature hindering the movement of electrons in the conductor. Finally, the thermistor is similar to the RTD, but instead of a metal such as platinum, a semiconductor is used to measure the resistance change as temperature changes. The difference between the outputs of the thermistor and the RTD is that the thermistor has a negative relationship with temperature: as the temperature increases in the thermistor, the resistance decreases. This is because of the temperature moving the electrons in the thermistor's semiconductor into the more conductive band, thus promoting electron movement and reducing

the resistance of the metal. Both the RTD and thermistor's outputs were recorded using two DMMS, one for each sensor, and the timing of the sensors to get to the steady state were done via a stopwatch.

After calibration, the response times of the sensors were tested. The response time of the sensors was found by introducing a step response by transferring the sensors from an ice bath to hot water and measuring the time it takes for the sensor to reach the steady state of 0°C. This time was used to find the response time constant of the sensor, which is detailed later (section 5).

Next, the transient heating/cooling of a thermocouple with an aluminium ball mass was experimented on. The ball mass was first submerged in ice water, and after reaching its steady state in the ice bath, the ball mass was placed into the hot water bath. The voltage change of this was recorded using the LabVIEW VI used when calibrating the regular thermocouple. Then, the ball mass was transferred from the hot water bath back into the ice bath, the voltage change being recorded again.

Finally, the conservation of energy was tested using the ball mass. The thermocouple was submerged in boiling water until it reached its steady state, then placed into a bath of water with a known volume. The temperature of the water was recorded using the thermometer before and after the ball mass was introduced.

Week two of this experiment began with retesting the response time of the RTD and thermistor this time using the DAQ module to take readings instead of a digital multi-meter. Both sensors were placed in boiling water until they reached steady state and then were immediately transferred to an ice bath to create the step change in temperature. These readings would then be compared to the original data from week 1 and discuss any differences in values.

The next part of the experiment consisted of measuring the temperature response of the aluminum sphere when it is subject to a step change in temperature. The aluminum sphere was first placed in boiling water and its initial temperature was recorded through its built-in thermocouple. Next, the aluminum sphere was removed from the boiling water and placed into another bucket containing either air or water at a much lower temperature than the boiling water to create the step change in temperature. The temperature response of the sphere was recorded by the built-in thermocouple through the LabVIEW VI to be used in our analysis.

This test procedure was preformed four times with buckets of different mediums: still air, moving air, still water, and flowing water. For still air, an anemometer was used to monitor the air speed to satisfy the validation of free convection criteria. To create moving air, an air-blower was used to force air convection over the aluminum sphere. For still water, a narrower bucket was filled with water in order to minimize the amount of possible water movement. The bucket of flowing water was created using a wider bucket of water that will be stirred at a constant rate by timing each stir revolution.

From the data collected, we will be able to calculate the heat transfer coefficient for each of the four cases studied. We will then compare them to the ranges of known heat transfer coefficients for air and water in free and forced convection and discuss why our calculated values do or do not fall within these ranges. Lastly, we will use the calculated heat transfer coefficients and fluid mechanics to estimate the fluid velocity.

3 Calibrations

The three temperature sensors (thermocouple, RTD, thermistor) used in this lab all needed to be calibrated. Before proceeding with the calibration of the sensors, the thermometer used for this calibration was verified using the reference temperatures of boiling water and ice.

The calibration of the sensors was carried out by mixing ice and boiling water to create solutions of a wide range of temperatures. The true temperature of these solutions was estimated via the thermometer, with the assumption that the solutions had a uniform temperature. Sensors were placed in each mixture,

including the boiling water and ice for additional data points, and the steady-state readings from the sensors were collected. A total of 5 data points were used for calibration to ensure goodness of linear fit. The data from this exercise (section 4) was subjected to linear analysis (section 5) to estimate the calibration constants needed to obtain reliable readings from the sensors.

4 Data

4.1 Calibration Data

Using the procedure outlined in section 3, the following data (figure 1) was collected for the three sensors. We note that the data corresponding to the thermocouple was collected as voltage readings via the DAQ module, whereas the resistances of the RTD and the thermistor were monitored through a digital multi-meter (DMM).

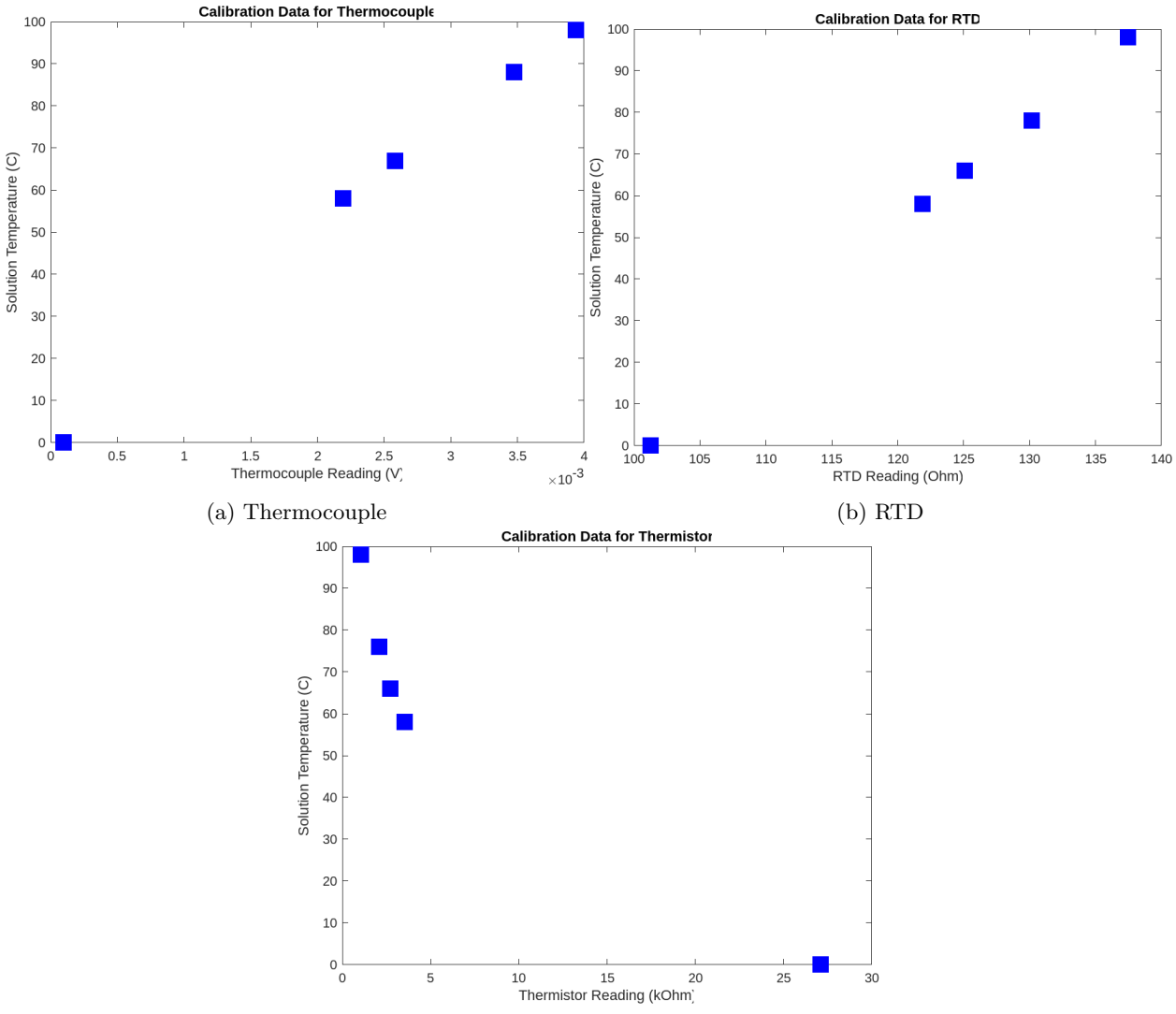

(a) Thermocouple

(b) RTD

(c) Thermistor

Figure 1: Raw data used for sensor calibration.

The comparison of thermometer readings in ice and boiling water showed that the range of readings

corresponding to the interval $0 - 100$C is $0 - 98$C. Subsequently, all data points were scaled in order to account for this discrepancy in thermometer readings. Lastly, using an additional wire of equal length, the wire resistance of the RTD was measured to be 0.3Ω.

4.2 Response Time Data

Using the method outlined in section 2, the data collected in order to calculate the response time of the thermocouple is listed in the graphs below:

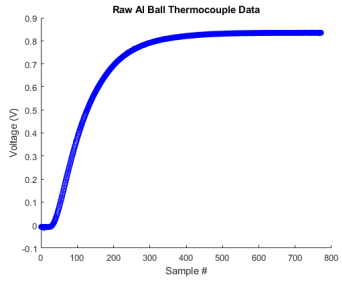

(a) Raw Al Thermocouple 1

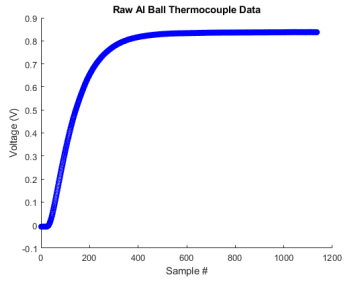

(b) Raw Al Thermocouple 2

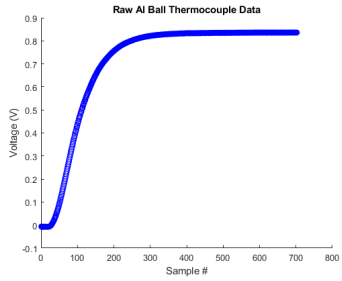

(c) Raw Al Thermocouple 3

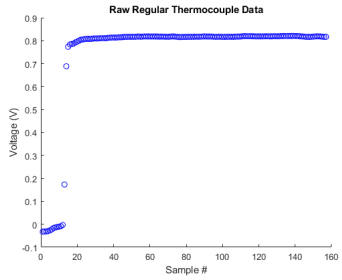

(d) Raw Reg Thermocouple 1

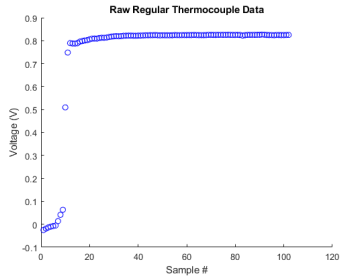

(e) Raw Reg Thermocouple 2

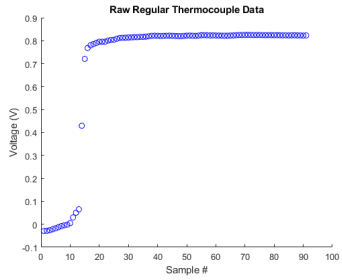

(f) Raw Reg Thermocouple 3

Figure 2: Raw graphs of thermocouple experiments

And the data for the response time for the RTD and thermistor are in the following tables:

Trial	**Time to steady state (s)**
Trial 1	37
Trial 2	37
Trial 3	39
Average	37.67

Table 1: RTD steady state time in seconds

Trial	**Time to steady state (s)**
Trial 1	27.5
Trial 2	25.5
Trial 3	26
Average	26.33

Table 2: Thermistor steady state time in seconds

In week 2 of the experiment, the response time test was repeated for both the RTD and thermistor using the DAQ module to take readings rather than a digital multi-meter for more accurate results due to its higher sampling rate. The data collected to calculate the response time are presented below:

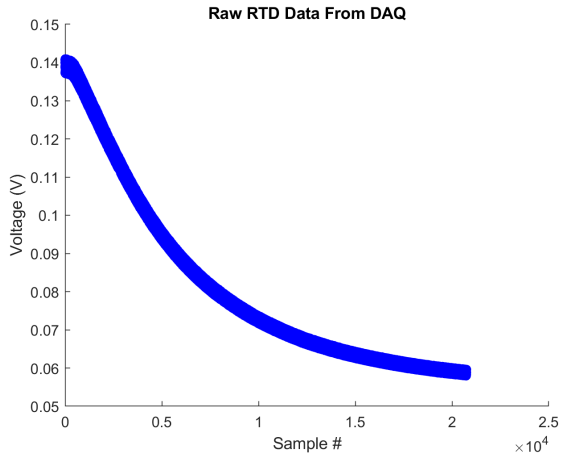

(a) Raw RTD Data From DAQ

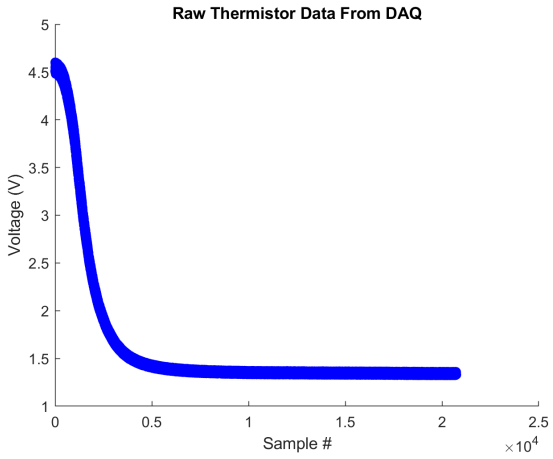

(b) Raw Thermistor Data From DAQ

The resulting response times as well as the uncertainty for the thermocouple, RTD, and thermistor are detailed in section 5.

4.3 Conservation of Energy Data

Using the method outlined in section 2, temperature data and volume measurements were taken to allow us to determine the degree of energy conserved through this heat transfer process. The initial and final temperatures were collected using the voltages from thermocouple sensor for the water bath and the built-in thermocouple for the aluminum sphere and converting them to temperature using the calibration factors explained in section 5.1. The volume of water used was measured with a graduated cylinder and the volume of aluminum was determined by measuring the diameter of the sphere which was 50.67mm. These temperatures and volumes along with the known densities and specific heats of the water bath and aluminum sphere were recorded as listed in the table below:

	Water Bath Data	**Aluminum Sphere Data**
Initial Temp, T_i [°C]	18.54	104.89
Final Temp, T_f [°C]	24.71	24.60
ΔT [°C]	6.17	80.29
Volume, V [L]	0.5	0.06812
Density, ρ [Kg/L]	1	2.71
Specific Heat, C [J/Kg K]	4184	900

Table 3: Temperature, volume, density, and specific heat of water bath and aluminum sphere.

These values will be used in calculating the heat energy gained and lost by the water bath and aluminum sphere as detailed in section 5.

4.4 Heat Transfer Coefficient

Using the method for week 2 outlined in section 2, the following data was collected in order to calculate the heat transfer coefficient of an aluminum sphere with varying cooling methods:

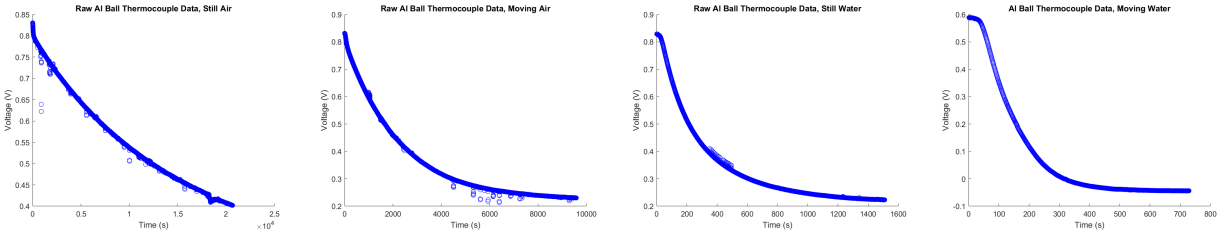

(a) Raw Still Air (b) Raw Moving Air (c) Raw Still Water (d) Raw Moving Water

Figure 4: Raw graphs of thermocouple convection experiments

The results were collected after exposing the sphere, embedded with a thermocouple, to a step-change of temperature under the shown convective conditions. We note that the cooling process of still air was substantially slower than the other processes, so the data collection was stopped earlier in the cooling process compared to the other data points.

5 Results

5.1 Calibration Results

The linearized form of the governing equations of the three sensor responses is summarized below. We observe that the semi-log representation of the thermistor resistance is used to give a linear account of this non-linear sensor.

$$\text{Thermocouple: } T = a_1[C] + a_2[\frac{C}{V}] \cdot V \tag{1}$$

$$\text{RTD: } T = a_1[C] + a_2[\frac{C}{\Omega}] \cdot R \tag{2}$$

$$\text{Thermistor: } \frac{1}{T} = a_1[\frac{1}{K}] + a_2[\frac{K}{ln(\Omega)}] \cdot ln(R) \tag{3}$$

$$\tag{4}$$

In order to process the calibration data, the collected data points were formatted according to these equations and the MATLAB function **Polyfit(x,y,n)** was used to obtain a linear fit. The corresponding coefficients along with the 95% interval of confidence (2 standard deviations) are provided in table 4; figure 5 contains a visual representation of this linear fit.

Property	**Thermocouple**	**RTD**	**Thermistor**
a_1	$-0.764C$	$-279C$	$0.0026K$
a_2	$2.61 \cdot 10^4 \frac{C}{V}$	$2.76\frac{C}{\Omega}$	$0.0003\frac{K}{k\Omega}$
Uncertainty	$3C$	$2C$	$3K$
Linearity (r)	0.999	1.00	0.999
Sensitivity	$4.28 \cdot 10^{-}5\frac{V}{C}$	$0.382\frac{\Omega}{C}$	$3.31 \cdot 10^3 \frac{k\Omega}{K}$ (See Text)
Sensitivity (Percentage)	$1.95\frac{\%V}{C}$	$0.314\frac{\%\Omega}{C}$	$1.00 \cdot 10^5 \frac{\%k\Omega}{K}$ (See Text)

Table 4: Results from linear regression analysis of the collected data.

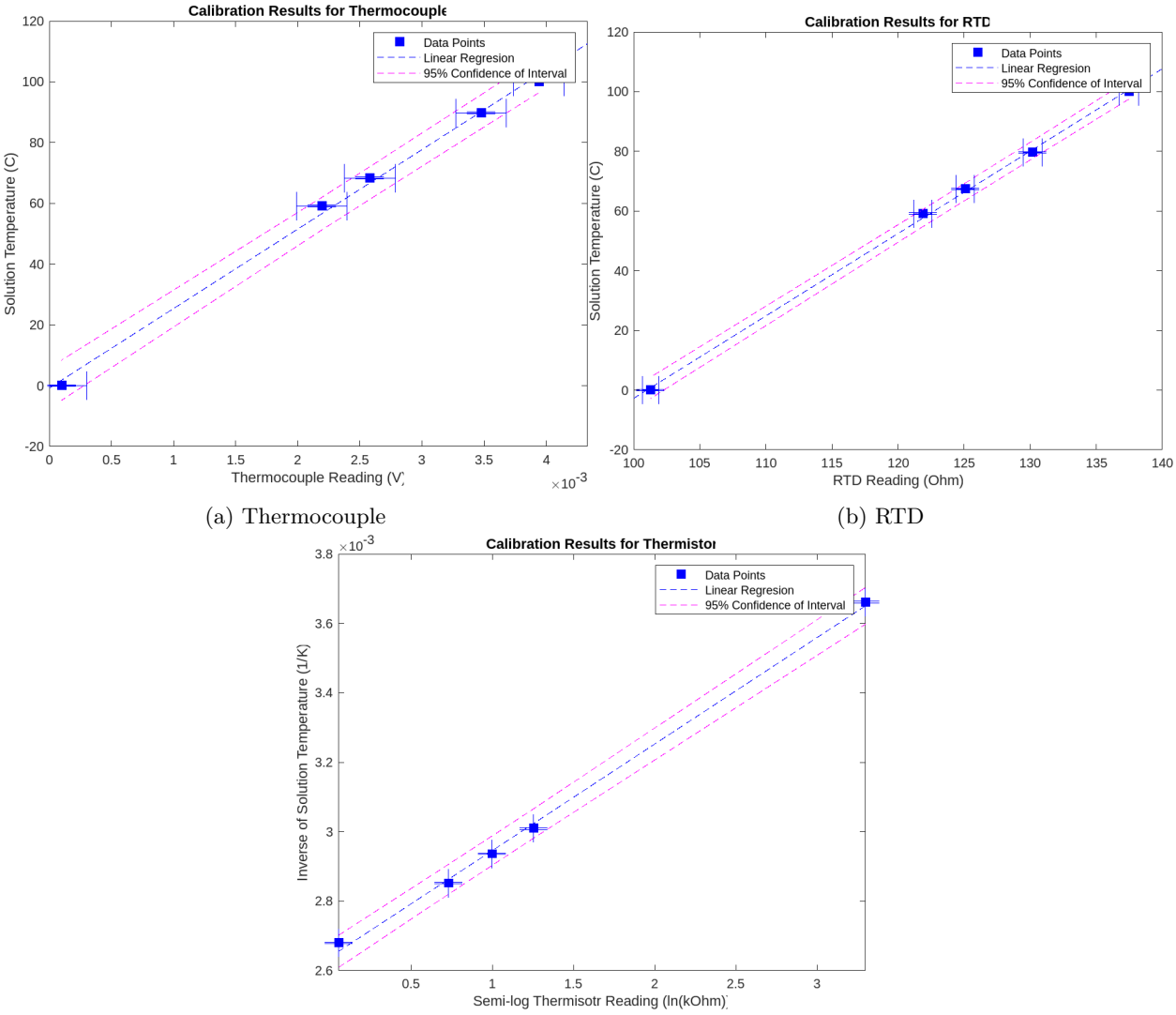

(a) Thermocouple

(b) RTD

(c) Thermistor

Figure 5: Processed calibration data with linear fits and 95% intervals of confidence.

Prior to line fitting, three processing adjustments were made to the data. First, the recorded thermocouple voltages were divided by the amplification factor of 207.7 which was supplied with the amplifying equipment used in the measurement system. Second, the wire resistance of the RTD was subtracted from the measured resistance readings. Lastly, the temperatures of the thermistor were converted to the Kelvin scale to avoid the artifacts of having a 0 reading in the $\frac{1}{T}$ term.

The treatment of uncertainty, both for linear fits and propagated error, is available in section 6. To evaluate the linearity of the resulting fits, we performed linear-regression analysis using the MATLAB function **corrcoef(A,B)**. The resulting correlation coefficients r are reported in table 4. This number indicates the strength of the linear relationship between the independent and dependent variables. Similarly, the table contains sensitivity analysis which was performed according to equations

$$\text{Sensitivity: } S = \frac{\Delta Output}{\Delta Input} \tag{5}$$

$$\text{Sensitivity (Percentage): } S = \frac{\%\Delta Output}{\Delta Input}. \tag{6}$$

$$\tag{7}$$

where the output is sensor voltage or resistance, and input is temperature. In both cases, sensitivity indicates the ability of a sensor to reflect small changes in the monitored state. When assessing sensitivities, we must note that the sensitivity reported for the thermistor is fundamentally different than the other two values, and has units of $(\frac{ln(R)}{\frac{1}{T}})$. On a voltage vs temperature scale, the sensor would have a non-constant sensitivity, largest at high temperatures and plateauing towards 0 at smaller temperatures. To demonstrate this, we present figure 6 which highlights two regimes of linear sensitivity for the thermistor with corresponding sensitivity values of $-0.0508\frac{k\Omega}{K}$ and $-0.399\frac{k\Omega}{K}$. sensitivity percentages of $-1.87\frac{\%k\Omega}{K}$ and $-11.4\frac{\%k\Omega}{K}$, and correlation coefficients 0.997 and 0.999. The implications of these figures are discussed in section 7.

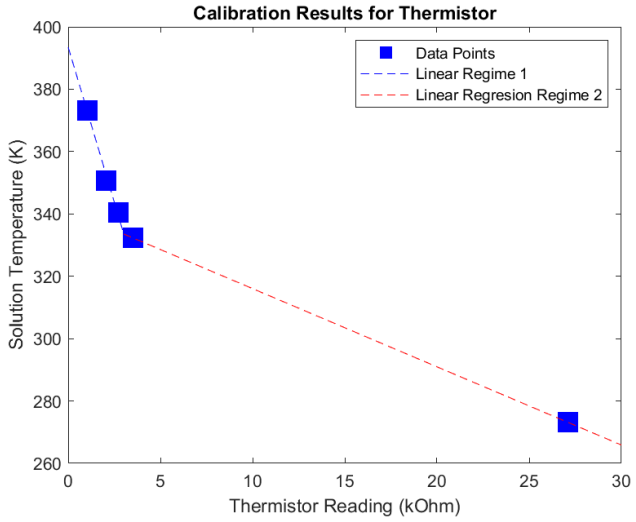

Figure 6: Processed calibration data showing two linear sensitivity regimes of the thermistor. Bounds of confidence and error bars are eliminated to avoid redundancy with previous figures.

5.2 Response Time Results

The response times of the thermocouple, RTD, and thermistor can be approximated by the lumped capacitance model, which assumes that the conductive cooling within the sensors is much more rapid than convective cooling at their surface. Thus, this model implies that the body has a constant temperature T which varies according to convection. Using this model, all three sensors demonstrate first order responses. As such, for the RTD and thermistor, the response of the two sensors can be modeled using the following:

$$\Theta(t) = \frac{T(t) - T_{\text{inf}}}{T_i - T_{\text{inf}}} = e^{-\frac{t}{\tau}} \tag{8}$$

Where Θ is the nondimensionalized temperature difference, $T(t)$, T_{inf}, T_i, are the current temperature,

temperature at steady state, and initial temperature respectively, t is the time, and τ is the response time constant. Due to the exponential term in this model, we can approximate an accurate time constant by taking 5τ, as it is when the response is 99.3% of the steady state. As such, we can rearrange equation (8) into:

$$\tau_{\text{RTD and thermistor}} = -\frac{t}{5ln(\Theta)} \tag{9}$$

To calculate the response time constants, the average time it took for the sensor to reach the steady state temperature was used.

For the thermocouple, due to measuring the voltage curve rather than the time it took for the sensor to get to steady state, a slightly different method was used. First, the voltage difference curve from the LabVIEW VI was converted from volts to °C using the calibration data found earlier. Next, the curve was nondimensionalized using the nondimensional temperature difference equation from (8), and finally linearized by taking the natural log of the data. Taking the line of best fit of this linearized data and finding the slope of said curve gives the time constant for the thermocouple, as:

$$ln(\Theta(t)) = ln(\frac{T(t) - T_{\text{inf}}}{T_i - T_{\text{inf}}}) = -\frac{t}{\tau_{\text{thermocouple}}}$$

Which can be rewritten as:

$$\tau_{\text{thermocouple}} = -\frac{t}{ln(\Theta(t))} \tag{10}$$

Meaning that the reciprocal of the slope of the line of best fit for the linearized thermocouple graphs is the time constant. After processing all of the thermocouple data to find the data set's time constant, the time constants were averaged out. This way of finding the time constant was done for the aluminum ball mass thermocouple as well.

The uncertainties of the response time constants were found using the equations outline later in section 6.2. Thus, the following table presents the resulting response time and uncertainty:

Sensor	**Response Time τ (s)**	**Uncertainty (s)**
Thermocouple (regular)	0.0921	± 0.5317
Thermocouple (Al ball)	7.7280	± 0.0167
RTD from DMM	1.9257	± 0.1537
Thermistor from DMM	1.3463	± 0.1092
RTD from DAQ	5.7438	± 0.3543
Thermistor from DAQ	1.0103	± 0.2187

Table 5: Response time and uncertainty of the sensors

The data for the temperature sensors mentioned in section 3 was cleaned up due to noise, and then formatted into a semilog plot to linearize it using the method mentioned earlier in the section. The line of best fit was then found using the MATLAB function **fit()**, the slope being the time constant, and looks as follows:

5.3 Conservation of Energy Results

The amount of heat energy gained by the water bath and lost by the aluminum sphere can be calculated using the heat energy equation:

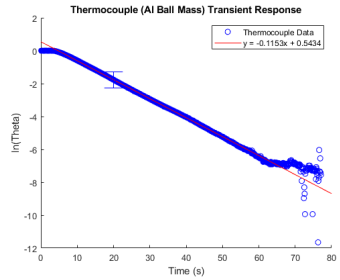

(a) Thermocouple (Al Ball)

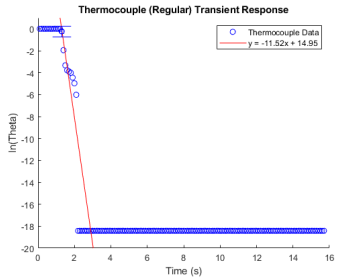

(b) Thermocouple (Regular)

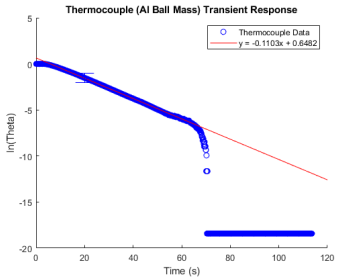

(c) Thermocouple (Al Ball)

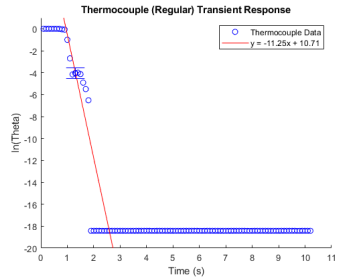

(d) Thermocouple (Regular)

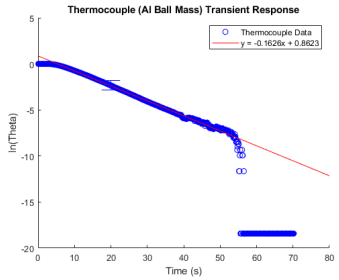

(e) Thermocouple (Al Ball)

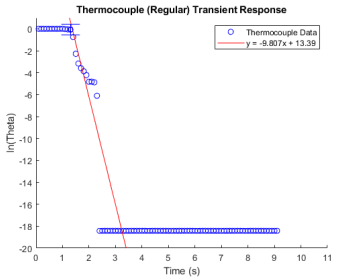

(f) Thermocouple (Regular)

Figure 7: Processed graphs of thermocouple experiments

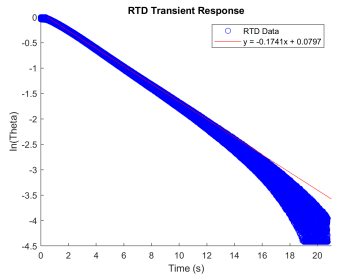

(a) RTD Data From DAQ

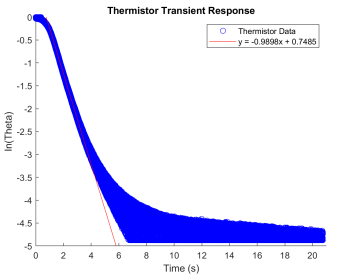

(b) Thermistor Data From DAQ

Figure 8: Processed graphs of RTD and Thermistor experiments

$$\Delta Q = mC\Delta T \tag{11}$$

The masses can be calculated through the equation $m = V\rho$. Using these equations and the data presented in section 4.3, the changes in heat energy can be calculated and are shown below:

	Water Bath	**Aluminum Sphere**
ΔQ [KJ]	$+12.91$	-13.34

Table 6: Amount of heat transfer between water bath and aluminum sphere

From these results we can see that the aluminum sphere lost more heat energy than what was gained by the water bath which suggests a discrepancy from the ideal conservation of energy. This heat was most likely lost to the environment but other reasons for this imbalance are discussed further in section 7.3. To calculate the percent of energy conservation in the system, the amount of heat energy gained by the water bath is divided by the amount of heat lost by the aluminum sphere. This shows that 96.8% of the energy

was conserved through this heat transfer process.

5.4 Heat Transfer Coefficient

5.4.1 Finding the Time Constant of the Cooling Process

The raw data from figure 9 was processed using MatLab's **movmean()** function in order to smooth the data out. Then, the voltage axis was nondimentionalized using the following equation:

$$\beta = \frac{V(t) - V_\infty}{V_0 - V_\infty} \tag{12}$$

Where V_0 is the initial voltage and V_∞ is the steady state voltage, or end voltage. This produces a nondimensional graph that can be linearized using a natural log function, which can then be used to find time constant τ of the system. This is similar to when the time constants were found in the previous section, as such the time constant equation looks like:

$$\tau = -\frac{t}{ln(\beta)} \tag{13}$$

Which is the reciprocal of the slope of the line of best fit of the linearized, nondimensionalized graph. We recall that this results from a lumped capacitance assumption. After fitting a line of best fit using the **fit()** MatLab function, the time constants were found and are listed in the following table:

Convection Mode	Response Time τ (s)	Uncertainty (s)
Still Air	937.21	$\pm$ 13.56
Moving Air	201.53	$\pm$ 1.18
Still Water	31.54	$\pm$ 0.48
Moving Water	9.38	$\pm$ 0.26

Table 7: Response time and uncertainty of the sensors

The uncertainty found and listed above is covered in detail in section 6.4.1. The graphs after processing looks as such:

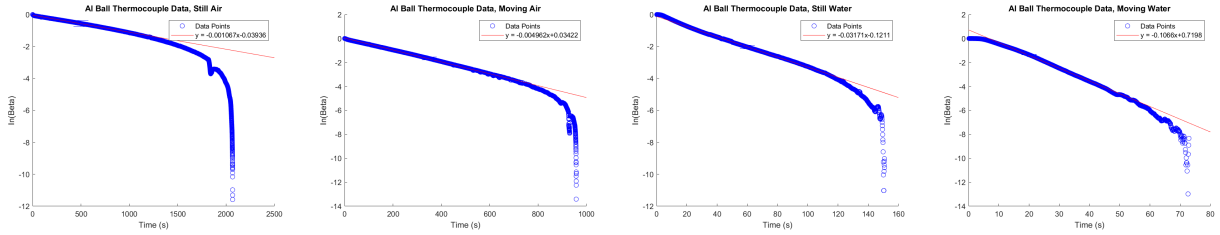

(a) Still Air (b) Moving Air (c) Still Water (d) Moving Water

Figure 9: Processed graphs of thermocouple convection experiments

5.4.2 Finding the Heat Transfer Coefficient

We recall the standard closed-form solution of transient lumped capacitance heat transfer that arises in the cooling of the aluminum sphere:

$$ln(\frac{T - T_{\text{inf}}}{T_i - T_{\text{inf}}}) = \frac{-hA}{mC_p}t \tag{14}$$

where the term $\frac{hA}{mC_p}$, composed of the heat transfer coefficient, the convective area, and the mass, is equivalent to the τ found above. Using this equation, we extract the following coefficients of heat transfer for the four cooling scenarios:

Convection Mode	**Heat Transfer Coefficient ($\frac{W}{m^2K}$))**	**Uncertainty ($\frac{W}{m^2K}$))**
Still Air	220	± 3
Moving Air	1020	± 6
Still Water	6530	± 100
Moving Water	21200	± 610

Table 8: Heat transfer coefficients extracted from step-response of aluminum sphere.

The uncertainty cited in table 8 arise from the propagation of the uncertainties in equation (14), addressed in section 6.4.1. In explaining the calculations, it should be pointed out that the specific heat capacity and density of aluminum were treated as constants, with tabulated values corresponding to 100°C adopted in calculations ($C_p = 9000[\frac{J}{kgK}]$, $\rho = 2710[\frac{kg}{m^3}]$).

5.4.3 Estimating the Fluid Velocity

The last step of the analysis for this lab consists of obtaining fluid velocity from the forced convection data. Once the heat transfer coefficient is known, the following set of equations

$$\begin{aligned} Nu &= \frac{hD}{k} \\ Nu &= 2 + 0.6Re^{\frac{1}{2}}Pr^{\frac{1}{3}} \\ Re &= \frac{\rho UD}{\mu} \end{aligned} \tag{15}$$

are used to find the Reynolds number and, subsequently, the fluid velocity. The results from this exercise are presented in table 9. The adopted values of dynamic viscosity for air and water are, respectively, $1.81 \cdot 10^-5[\frac{kg}{ms}]$ and $8.90 \cdot 10^-4[\frac{kg}{ms}]$. Similarly, the prandtl numbers for air and water were found to be 0.701 and 1.76 at 100°C. Lastly, the density and thermal conductivity of the fluids were estimated at $1.225[\frac{kg}{m^3}]$ and $31.62[\frac{mW}{mk}]$ for air and $997[\frac{kg}{m^3}]$ and $677[\frac{mW}{mk}]$ for water.

Convection Mode	**velocity ($\frac{m}{s}$)**	**Uncertainty ($\frac{m}{s}$)**
Moving Air	2750	± 30
Moving Water	90.5	± 5

Table 9: Fluid velocities extracted from step-response of aluminum sphere under forced convection.

We observe that the velocities are nonphysically large. The heat transfer coefficients are also larger than the empirically available, which may point to a systematic error in the measurements. This consideration is further discussed in section 7.

6 Uncertainty

6.1 Calibration Uncertainty

The uncertainty in the calibration analysis stems from two sources: propagation of uncertainty from measurement inaccuracies, and uncertainty associated with the imperfect linear fit. The former phenomenon stems from the instrument limitations:

$$\text{DAQ Voltages: } \Delta = 115\text{ppm} \cdot \text{Reading} + 406\mu V \tag{16}$$

$$\text{DMM Resistance (RTD): } \Delta = 0.8\% \cdot \text{Reading} + 4 \cdot \text{Resolution} \tag{17}$$

$$\text{DMM Resistance (Thermistor): } \Delta = 0.8\% \cdot \text{Reading} + 2 \cdot \text{Resolution} \tag{18}$$

These equations are used to generate the error bars in figure 5. When formatting the data for the thermistor as a semilog plot, we used the following equations:

$$\text{Propagation of Uncertainty} = \sqrt{\sum_{i=1}^{n} (\frac{\delta f}{\delta x_i} \Delta x_i)^2} \tag{19}$$

$$\Delta(ln(x)) = \frac{1}{x} \cdot \Delta x \tag{20}$$

$$\Delta(\frac{1}{x}) = \frac{1}{x^2} \cdot \Delta x \tag{21}$$

In order to asses the second source of uncertainty, we used the MATLAB function **Polyval(p,x)**, which provided the standard deviation for the linear fit **p**.

From the figures, it is evident that the contribution from both of these sources of error is comparable. In the table 4, the uncertainty of the curve fit is provided because it captures the variation between the data points.

6.2 Response Time Uncertainty

The uncertainty of the response time can be calculated using the error propagation equation according to equation (19). As such, for the RTD and thermistor, there are multiple sources of uncertainty. The first source is the DMM resistance uncertainty, which was found in the previous section. The second source is with the response time itself, where the response time can vary away from the true time. This standard deviation of the mean can be found using the following equation:

$$\Delta\bar{x} = \sqrt{\frac{1}{n(n-1)} \sum_{i=1}^{n} (x_i - \bar{x})^2} \tag{22}$$

This standard deviation is treated as $\Delta\bar{x}$ when using equation (19). Next, the uncertainty of the dimensionless temperature difference $\Delta\Theta$ had to be found. This is found by taking half of the smallest unit of measure on the thermometer, which comes out to be $\Delta T = .5°\text{C}$. This uncertainty from the thermometer is then plugged into the dimensionless temperature gradient equation explained in equation (8). With all of the possible uncertainties taken to account, the error propagation for the RTD and thermistor as can be generally written

as:

$$\Delta\tau_{\text{RTD and thermistor}} = \sqrt{(\frac{\Delta\bar{x_i}}{5ln(\Theta)})^2 + (\frac{\Theta(\Delta\Theta)\bar{x_i}}{5})^2} \tag{23}$$

For the thermocouples, two additional sources of uncertainty needs to be taken to account. The first is the DAQ, again discussed in an earlier section. The second source is from the linear fit when finding the thermocouple's line of best fit. The uncertainty from this linear fit model can be expressed with the following:

$$\Delta m = s\sqrt{\frac{n}{n\sum_i x_i^2 - (\sum_i x_i)^2}} \tag{24}$$

$$\Delta b = s\sqrt{\frac{\sum_i x_i^2}{n\sum_i x_i^2 - (\sum_i x)^2}} \tag{25}$$

$$s = \sqrt{\frac{\sum_i y_i^2 - \frac{1}{n}(\sum_i y_i)^2 - m(\sum_i x_i y_i - \frac{1}{n}\sum_i x_i \sum_i y_i))}{n-2}} \tag{26}$$

Where Δm is the slope's uncertainty, Δb is the uncertainty of the offset, m is the slope of the linear fit, and n is the total number of data points used. Since the averages of the time constants were taken using this linear fit method, the standard deviation of the mean was found as well. These two uncertainties were combined for an overall uncertainty for the thermocouples. Further propagation is not needed as only the voltage output of the thermocouples were measured, whereas for the RTD and thermistor, temperature (in voltage) and time was measured.

6.3 Conservation of Energy Uncertainty

The uncertainty in the conservation of energy calculations is derived through the propagation of uncertainty from inaccuracies in the measurement devices and the thermocouple calibration uncertainty.

The thermocouple calibration uncertainty equation, as shown in equation (16), is used to determine the uncertainty in the initial and final temperature readings taken by the thermocouple. These uncertainties are then used with the propagation of uncertainty equation, as shown in equation (19), to calculate the uncertainty in the change in temperature of each material.

The volume of water used was measured using a graduated cylinder so the uncertainty in this measurement was half of the smallest measurement mark. The volume of the aluminum sphere was calculated using the diameter of the sphere measured using calipers. The uncertainty of the calipers is half of its smallest measurement mark and using the propagation of uncertainty equation, the uncertainty of the sphere's volume can then be calculated.

The uncertainty of the mass of water and aluminum used in this experiment is also calculated using the propagation of uncertainty equation from the volume and known densities of water and aluminum. Since the density and specific heat of each material are known values and not values we tested for we will assume there is no uncertainty to their values.

Using the calculated mass and temperature change uncertainties along with the known values of specific heat, we can then calculate the uncertainty in the amounts of heat transferred between the water bath and aluminum sphere. Since the amount of heat transferred between the water and sphere is representative of the degree of conservation of energy, the uncertainty in the amount of heat transferred is representative of our uncertainty in the degree of conservation of energy. The calculated values of each of these uncertainties

are listed in the table below.

	Water Bath Uncertainties	**Aluminum Sphere Uncertainties**
Initial Temp, T_i [°C]	4.24e−4	5.03e−4
Final Temp, T_f [°C]	4.29e−4	4.29e−4
ΔT [°C]	6.03e−4	6.61e−4
Volume, V [L]	5e−3	8.07e−5
Mass, m [Kg]	5e−3	2.19e−4
ΔQ [KJ]	1.29e−1	1.58e−2

Table 10: Temperature and volume uncertainties of water bath and aluminum sphere.

6.4 Heat Transfer Coefficient Uncertainty

6.4.1 Uncertainty in Time Constant

There are two sources of uncertainty in the convection experiment. The first is from the DAQ voltage reading, which was covered previously in section 6.1. When applying this error into the data, however, it was found that it was minute compared to the other source of data, so it was omitted for brevity. The more major source of this error comes from the slope error when taking the line of best fit of the linearized data. This was covered in section 6.2, and applied when finding the uncertainty from taking the linear slope fit.

6.4.2 Propagation of Uncertainty for Coefficients of Heat Transfer

The bulk of analysis for propagation of uncertainty relies on equation (21). For the heat transfer coefficient, this expression yields the following set of formula:

$$\Delta h = \sqrt{(\frac{C_p}{A\tau}\cdot\rho\cdot\Delta V)^2+(\frac{mC_p}{A^2\tau}\cdot\Delta A)^2+(\frac{mC_p}{A\tau^2}\cdot\Delta\tau)^2} \tag{27}$$

Where:

$$\Delta A = 8\pi r\Delta r \tag{28}$$

$$\Delta V = 4\pi r^2\Delta r \tag{29}$$

$$\tag{30}$$

Recall that the mass was estimated as a multiplication of density by volume. Additionally, we make the assumption that the uncertainty of the tabulated values (density, specific heat capacity) are far smaller than experimental uncertainties, so the corresponding terms are discarded from the calculations. Lastly, the uncertainty of the measured diameter was found as half of the smallest decimal measured by the caliper, namely $0.005mm$.

6.4.3 Propagation of Uncertainty in Calculation of Fluid Velocities

Similar to the above sections, the equation for the propagation of uncertainty for fluid velocities was found to be the following.

$$\Delta Nu = \sqrt{(\frac{d \cdot \Delta h}{k})^2 + (\frac{h \cdot \Delta d}{k})^2} \tag{31}$$

$$\Delta Re = \frac{2^{\frac{Nu-0.2}{0.6}}}{Pr^{\frac{2}{3}} \cdot 0.6} \cdot \Delta Nu \tag{32}$$

$$\Delta U = \sqrt{(\frac{\mu \cdot \Delta Re}{\rho d})^2 + (\frac{Re\mu \cdot \Delta d}{\rho d^2})^2} \tag{33}$$

Note that three stages of error propagation are accounted for: the propagation of uncertainty in finding Nu from h, and the propagation of uncertainty in finding Re from Nu, and, finally, the propagation of uncertainty in finding v from Re. As before, the tabulated values of the Prandtl number and the dynamic viscosities were taken to be free of uncertainty. The MATLAB script used for these calculations is featured in the appendix.

7 Discussion

7.1 Calibration Linearity and Sensitivity

Before discussing the linearity and sensitivity of the calibration results, we reiterate that it is desirable to have instrument uncertainties that are orders of magnitude smaller than the uncertainty of the linear fit. In reporting the uncertainty in section 6, the focus is shifted to the latter source of uncertainty because it captures the deviation of data points from linear behavior. However, the integrity of the reported data would be greater if instruments with less uncertainty were used. In the case of the thermistor data, the relative uncertainty of the DAQ is amplified by the fact that the input signal is minuscule prior to amplification.

Comparing the linearity and sensitivity of the sensors highlights their comparative performance. While the RTD has the greatest correlation coefficient, all sensors display a largely linear behavior over the measured temperatures ($R > 0.99$) - in the case of thermistor, this linear response is an artifact of the logarithmic formulation. The sensitivity, however, is not uniform: the thermocouple ($S = 1.95\%$) has a larger sensitivity than the RTD ($S = 0.314\%$). Focusing on the thermistor, the non-constant linear sensitivity implies that the monitored temperature range informs whether thermistor is adequately sensitive. For instance, if a measurement is being made at very high temperatures and high sensitivity is desired, the thermistor may be a good candidate. In contrast, if high-sensitivity measurements across a large range of temperatures are desired, the thermocouple is a stronger candidate. Lastly, we remark that the linearity and sensitivity estimates provided for the individual thermistor regimes are subject to greater uncertainty because only a few data points were available for each set of calculations.

7.2 Response Time Trends

As stated earlier, the focus of the uncertainty is shifted towards experimental uncertainty and not instrumental uncertainty. With that aside, comparing the response times of all of the sensors shows that the fastest response time is with the regular thermocouple. The response time of the regular thermocouple is almost like a zero order response, where it almost immediately went to the target temperature based on the raw data. If the response time is the priority in selecting a sensor, then an exposed thermocouple will be sufficient as it will immediately sense the change in temperature and change its voltage output. However, regular thermocouple has an incredibly high uncertainty compared to the other sensors, being roughly 5x larger than the other uncertainties. Thus, the regular thermocouple may be fast responding, but vastly

less accurate than the rest. If accuracy is needed, then the aluminum ball thermocouple performs the best, having the lowest uncertainty than the rest. For both accuracy and response time, the thermistor offers a more balanced performance between the two. It responded to temperature changes faster than the RTD and aluminum ball thermocouple, and is more accurate than the regular thermocouple and RTD. This is especially apparent when viewing the response time readings taken by the DAQ module in week 2 of the experiment. Due to the DAQ module having a higher sampling rate than the digital multi-meter used in week 1 and because of the large number of data points collected, the thermistor can be seen to have a response time of less than a quarter of that of the RTD. If response time and accuracy is needed, then the the thermistor is the best performing sensor for those needs.

7.3 Remarks on Conservation of Energy

The 96.8% energy conservation between the water bath and aluminum sphere does not fully satisfy the ideal conservation of energy requirements. While inaccuracies in the thermocouples and the overall uncertainties calculated may have played a roll in this discrepancy, this was most likely due to the imperfections in the test setup causing a small amount of heat energy to get absorbed by the surroundings. Although this test was preformed in an insulated bucket to improve the amount of heat contained in the system, no system can be made completely perfect and so some amount of heat energy was bound to be lost.

One other factor considered was the time it takes for heat to propagate through a medium. Since the sphere's built-in thermocouple was in the very center of the sphere, it would be much warmer by the end of the experiment than the average temperature of the sphere. Likewise, since the other thermocouple was submerged in non-moving water it is unlikely that there would have been an even temperature distribution throughout the entire bucket. The water closer to the hot sphere would be much warmer than the water further away from it and it would have taken much longer than the couple minutes this test lasted for for there to be a completely uniform temperature distribution. Since our heat transfer calculations stems from our temperature data, this could have further influenced our conservation of energy calculations.

7.4 Heat Transfer Coefficient

The results collected from the aluminum sphere show a wide range of time constants (τ) based on the mode of convection. It can be seen that cooling the sphere naturally using air as a medium produces the highest time constant from the rest. This is expected as natural convection is the slowest mode of cooling an object down. The lowest time constant was with moving water, as it emulates forced convection with water. Water itself can dissipate heat better than air, and forced convection cools objects down faster too. As such, a large jump between the time constants of the still air and moving water can be seen.

Comparing the results in table 8 to the commonly accepted ranges of heat transfer coefficients suggests that the results obtained in this experiment overestimated the heat transfer coefficient of water and air by, at most, an order of magnitude. This is further reflected in the nonphysically large velocities obtained in table 9. This discrepancy can be explained by the fact that the aluminum sphere was attached to a rod of non-negligible surface area. The rod was subject to convection along with the sphere, which resulted in more rapid cooling than what would be predicted by the model and, subsequently, large heat transfer coefficients. This conjecture is further supported by the fact that the air velocity was orders of magnitude larger than water velocity; because the rod section was fully suspended in air but not water, this source of error would affect the air calculations disparately. In addition, the rod was held by clamps or a user, which added a conductive path that further skewed the predicted coefficients. These unaccounted modes of heat transfer act as a source of systematic error in the experiment that could be alleviated in post-processing by modeling

the heat transfer through the rod.

8 Appendix A: MATLAB Data Processing Script for Calibrations

```
%% Data processing for calibration of temperature Sensors
%Last Edit: VB 10/18
%ME105, Vedad Bassari, Michael Howo, Connor Tang
clc; clear; close all;

TC_V = [0.818;0.722;0.536;0.455;0.02]; %Thermocouple voltage radings [V]
TC_V = TC_V./207.7; %Accounting for amplification
TC_T = [98;88;67;58;0]; %Thermocouple temeperature [C]
RTD_R = [137.5;130.2;125.1;121.9;101.3]; %RTD resistance readings [Ohm]
RTD_R = RTD_R - 0.03; %Accounting for wire resistance
RTD_T = [98;78;66;58;0]; %RTD temperature readings [C]
T_R = [1.054;2.074;2.714;3.52;27.1]; %Thermistor resistance readings [Ohm]
T_T = [98;76;66;58;0]; %Thermistor temperature readings [C]

%Plot data for thermocouple
figure();
plot(TC_V,TC_T,'bs','MarkerSize',15,'MarkerFaceColor',[0 0 1]);
title('Calibration Data for Thermocouple');
ylabel('Solution Temperature (C)');
xlabel('Thermocouple Reading (V)');

%Plot data for RTD
figure();
plot(RTD_R,RTD_T,'bs','MarkerSize',15,'MarkerFaceColor',[0 0 1]);
title('Calibration Data for RTD');
ylabel('Solution Temperature (C)');
xlabel('RTD Reading (Ohm)');

%Plot data for thermistor
figure();
plot(T_R,T_T,'bs','MarkerSize',15,'MarkerFaceColor',[0 0 1]);
title('Calibration Data for Thermistor');
ylabel('Solution Temperature (C)');
xlabel('Thermistor Reading (kOhm)');

%Adjustment of thermometer readings
TC_T = TC_T.*(100./98);
RTD_T = RTD_T.*(100./98);

%Eliminate edge cases from the thermistor calibration
T_R = [1.054;2.074;2.714;3.5;27.1]; %Thermistor resistance readings [kOhm]
T_T = [98;76;66;58;0]; %Thermistor temperature readings [C]
```

```
T_T = T_T.*(100./98);
T_T = T_T + 273.15; %Converting to Kelvin
log_T_R = log(T_R); %Arrays formatted for semi-log plotting
log_T_T = 1./(T_T);

%Error Propagation
d_TC_T = zeros(5,1) + 0.5; %Uncertainty of thermometer readings
d_RTD_T = zeros(5,1) + 0.5;
d_T_T = zeros(5,1) + 0.5;
d_T_T = d_T_T.*(1./(T_T.^2));
d_TC_V = ((115./(10.^6)).*TC_V) + (406.*(10.^-6)); %Uncertainty of DAQ
d_RTD_R = ((0.8./100).*RTD_R) + (4.*0.1); %Uncertainty of DMM
d_T_R = ((0.8./100).*T_R) + (2.*0.001);
d_T_R = d_T_R*(1/T_R);
d_T_R = d_T_R(:,4);

%Line fitting
[TC_fit,TC_fit_s] = polyfit(TC_V,TC_T,1); %Obtain linear fit
%Evaluate uncertainty of linear fit
[TC_y_fit,TC_delta] = polyval(TC_fit,TC_V,TC_fit_s);
TC_fit_stdev = mean(TC_delta);
TC_r = corrcoef(TC_V,TC_T); %Linearity: correlation of coefficient
%Sensitivity: absolute and percentage-wise
TC_S = ((TC_V(end-1)-TC_V(1))./(TC_T(end-1)-TC_T(1)));
TC_S_p = (((TC_V(end-1)-TC_V(1))./(TC_V(end-1)).*100)./...
    (TC_T(end-1)-TC_T(1)));

%Plot data for thermocouple
figure();
plot(TC_V,TC_T,'bs','MarkerSize',8,'MarkerFaceColor',[0 0 1]);
title('Calibration Results for Thermocouple');
ylabel('Solution Temperature (C)');
xlabel('Thermocouple Reading (V)');
hold on;
x = linspace(0,0.9./207.7);
TC_line = TC_fit(1).*x + TC_fit(2);
plot(x,TC_line,'--b','LineWidth',0.5)
hold on;
plot(TC_V,TC_y_fit+2*TC_delta,'m--',TC_V,TC_y_fit-2*TC_delta,'m--')
legend('Data Points','Linear Regresion','95% Confidence of Interval');
errorbar(TC_V,TC_T,-d_TC_T./2,d_TC_T./2,-d_TC_V./2,d_TC_V./2,'bs',...
    'CapSize',20,'HandleVisibility','off')
xlim([0 0.9./207.7]);
```

```
%Line fitting
[RTD_fit,RTD_fit_s] = polyfit(RTD_R,RTD_T,1); %Obtain linear fit
%Evaluate uncertainty of linear fit
[RTD_y_fit,RTD_delta] = polyval(RTD_fit,RTD_R,RTD_fit_s);
RTD_fit_stdev = mean(RTD_delta);
RTD_r = corrcoef(RTD_R,RTD_T); %Linearity: correlation of coefficient
%Sensitivity: absolute and percentage-wise
RTD_S = ((RTD_R(end-1)-RTD_R(1))./(RTD_T(end-1)-RTD_T(1)));
RTD_S_p = (((RTD_R(end-1)-RTD_R(1))./(RTD_R(end-1)).*100)./...
    (RTD_T(end-1)-RTD_T(1)));

%Plot data for RTD
figure();
plot(RTD_R,RTD_T,'bs','MarkerSize',8,'MarkerFaceColor',[0 0 1]);
title('Calibration Results for RTD');
ylabel('Solution Temperature (C)');
xlabel('RTD Reading (Ohm)');
hold on;
x = linspace(100,140);
RTD_line = RTD_fit(1).*x + RTD_fit(2);
plot(x,RTD_line,'--b','LineWidth',0.5)
hold on;
plot(RTD_R,RTD_y_fit+2*RTD_delta,'m--',RTD_R,RTD_y_fit-2*RTD_delta,'m--');
legend('Data Points','Linear Regresion','95% Confidence of Interval');
errorbar(RTD_R,RTD_T,-d_RTD_T./2,d_RTD_T./2,-d_RTD_R./2,d_RTD_R./2,'bs',...
    'CapSize',20,'HandleVisibility','off')
xlim([100 140]);

%Line fitting
[T_fit,T_fit_s] = polyfit(log_T_R,log_T_T,1); %Obtain linear fit
%Evaluate uncertainty of linear fit
[T_y_fit,T_delta] = polyval(T_fit,log_T_R,T_fit_s);
T_fit_stdev = mean(T_delta);
T_r = corrcoef(log_T_R,log_T_T); %Linearity: correlation of coefficient
%Sensitivity: absolute and percentage-wise
T_S = ((log_T_R(end)-log_T_R(1))./(log_T_T(end)-log_T_T(1)));
T_S_p = (((log_T_R(end)-log_T_R(1))./(log_T_R(end)).*100)./...
    (log_T_T(end)-log_T_T(1)));

%Plot data for thermistor
figure();
plot(log_T_R,log_T_T,'bs','MarkerSize',8,'MarkerFaceColor',[0 0 1]);
```

```
title('Calibration Results for Thermistor');
ylabel('Inverse of Solution Temperature (1/K)');
xlabel('Semi-log Thermisotr Reading (ln(kOhm))');
hold on;
x = linspace(0.05,3.30);
T_line = T_fit(1).*x + T_fit(2);
plot(x,T_line,'--b','LineWidth',0.5)
hold on;
plot(log_T_R,T_y_fit+2*T_delta,'m--',log_T_R,T_y_fit-2*T_delta,'m--')
legend('Data Points','Linear Regresion','95% Confidence of Interval');
errorbar(log_T_R,log_T_T,-d_T_T./2,d_T_T./2,-d_T_R./2,d_T_R./2,'bs',...
    'CapSize',20,'HandleVisibility','off')
xlim([0.05 3.30]);

%Line fitting
[T_fit_A,T_fit_s_A] = polyfit(T_R(1:3),T_T(1:3),1); %Obtain linear fit
[T_fit_B,T_fit_s_B] = polyfit(T_R(4:5),T_T(4:5),1); %Obtain linear fit
%Evaluate uncertainty of linear fit
[T_y_fit_A,T_delta_A] = polyval(T_fit_A,T_R(1:3),T_fit_s_A);
[T_y_fit_B,T_delta_B] = polyval(T_fit_B,T_R(4:5),T_fit_s_B);
T_fit_A_stdev = mean(T_delta_A);
T_fit_B_stdev = mean(T_delta_B);
T_r_A = corrcoef(T_R(1:3),T_T(1:3)); %Linearity: correlation of coefficient
T_r_B = corrcoef(T_R(4:5),T_T(4:5)); %Linearity: correlation of coefficient
%Sensitivity: absolute and percentage-wise
T_S_A = ((T_R(3)-T_R(1))./(T_T(3)-T_T(1)));
T_S_B = ((T_R(5)-T_R(4))./(T_T(5)-T_T(4)));
T_S_A_p = (((T_R(3)-T_R(1))./(T_R(3)).*100)./...
    (T_T(3)-T_T(1)));
T_S_B_p = (((T_R(5)-T_R(4))./(T_R(4)).*100)./...
    (T_T(5)-T_T(4)));

%Plot data for thermistor
figure();
plot(T_R,T_T,'bs','MarkerSize',15,'MarkerFaceColor',[0 0 1]);
title('Calibration Results for Thermistor');
ylabel('Solution Temperature (K)');
xlabel('Thermistor Reading (kOhm)');
hold on;
xA = linspace(0,3);
T_line_A = T_fit_A(1).*xA + T_fit_A(2);
plot(xA,T_line_A,'--b','LineWidth',0.5)
hold on;
```

```
xB = linspace(3,30);
T_line_B = T_fit_B(1).*xB + T_fit_B(2);
plot(xB,T_line_B,'--r','LineWidth',0.5)
legend('Data Points','Linear Regime 1','Linear Regresion Regime 2');
xlim([0 30]);
```

9 Appendix B: MATLAB Data Processing Script for Response Time Analysis

```
clc; clearvars;

%% thermocouple uncertainty stuff
SR_response = [.1153;.1103;.1626];
TC_response = [11.52;11.25;9.807];
SR_error = [.0002; .0003; .0006];
SR_mean_error = [0; 0; 0];

n = 3;

mean_SR_Response = mean(SR_response);
mean_TC_Response = mean(TC_response);
SD_SR = sqrt(1/(n*(n-1))*sum((SR_response-mean_SR_Response).^2));
SD_TC = sqrt(1/(n*(n-1))*sum((TC_response-mean_TC_Response).^2));

for i = 1:n
    SR_mean_error(i) = SR_error(i)/SR_response(i);
end

uncert_SR = sqrt(sum(SR_mean_error.^2)/n + (SD_SR/mean_SR_Response)^2);

%% RTD and thermistor stuff

% temperatures measured in degrees Celsius
T_0 = 0;
T_f = 98; %final temperature and temperature at steady state

RTD_response = [37;37;39];
therm_response = [27.5;25.5;26];

n = length(RTD_response);

% assuming that the response time is at 5*tau, where they were at steady
% state, the following equation is used: Omega(t) = e^(-t/5tau)

mean_RTD_Response = mean(RTD_response);
mean_therm_Response = mean(therm_response);
SD_RTD = sqrt(1/(n*(n-1))*sum((RTD_response-mean_RTD_Response).^2));
SD_therm = sqrt(1/(n*(n-1))*sum((therm_response-mean_therm_Response).^2));

nonDimTemp = (98-100)/(0-100);
nonDimTemp_uncertainty = (.5-100)/(0-100);
```

```
tau_RTD = -(mean_RTD_Response/(5*log(nonDimTemp)));
tau_therm = -(mean_therm_Response/(5*log(nonDimTemp)));

tau_RTD_uncert = sqrt((SD_RTD/(5*log(nonDimTemp)))^2 +...
(nonDimTemp*nonDimTemp_uncertainty*mean_RTD_Response/5)^2);
tau_therm_uncert = sqrt((SD_therm/(5*log(nonDimTemp)))^2 +...
(nonDimTemp*nonDimTemp_uncertainty*mean_therm_Response/5)^2);

%% thermocouples
clc; clearvars;

TC_data = readmatrix("SR5.txt");
TC_data2 = readmatrix("TR4.txt");
TC_SR = TC_data(:,2);
TC_TC = TC_data2(:,3);
a1 = -.764;
a2 = 2.61*10^4;
amp_factor_SR = 216.4;
amp_factor_TC = 207.7;

%{
figure(); hold on;
plot(TC_SR, "blueo");
title("Raw Al Ball Thermocouple Data");
xlabel("Sample #");
ylabel("Voltage (V)");
hold off;
figure(); hold on;
plot(TC_TC, "blueo");
title("Raw Regular Thermocouple Data");
xlabel("Sample #");
ylabel("Voltage (V)");
hold off;
%}

TC_SR_temp = a1 + a2.*(TC_SR./amp_factor_SR);
TC_TC_temp = a1 + a2.*(TC_TC./amp_factor_TC);
TC_length = length(TC_TC_temp);

i = 0;
j = 0;
while i < length(TC_SR_temp)
```

```
    i = i+1;
    if(TC_SR_temp(i) < 0)
        TC_SR_temp(i) = 0.000001;
    elseif(TC_SR_temp(i)>100)
        TC_SR_temp(i) = 99.999999;
    end
end
while j < TC_length
    j = j+1;
    if(TC_TC_temp(j) < 0)
        TC_TC_temp(j) = 0.000001;
    end
    if(TC_TC_temp(j) > 100)
        TC_TC_temp(j) = 99.999999;
    end
    %{
    if(j > 180)
        TC_TC_temp(j) = [];
        TC_length = TC_length - 1;
        j = j-1;
    end
    %}
end

TC_SR_nondim = (TC_SR_temp-100)/(0-100);
TC_TC_nondim = (TC_TC_temp-100)/(0-100);

TC_SR_lin = log(TC_SR_nondim);
TC_TC_lin = log(TC_TC_nondim);

TC_SR_time = [1:1:length(TC_SR_lin)]'./10;
TC_TC_time = [1:1:length(TC_TC_lin)]'./10;

TC_SR_data = [TC_SR_time TC_SR_lin];
TC_TC_data = [TC_TC_time TC_TC_lin];

TC_SR_range = [50:1:500]';
TC_SR_fit = fit(TC_SR_data(TC_SR_range, 1), TC_SR_data(TC_SR_range, 2), 'poly1');
TC_TC_range = [13:1:24]';
TC_TC_fit = fit(TC_TC_data(TC_TC_range, 1), TC_TC_data(TC_TC_range, 2), 'poly1');

SRdataPoint = 200;
SR_V = TC_SR(SRdataPoint);
```

```
pre_d_SR_V = (a1 + a2.*((((115./(10.^6)).*SR_V) + (406.*(10.^-6)))./amp_factor_SR));
d_SR_V = 1/((pre_d_SR_V-100)/(0-100));

TCdataPoint = 13;
TC_V = TC_TC(TCdataPoint);
pre_d_TC_V = (a1 + a2.*((((115./(10.^6)).*TC_V) + (406.*(10.^-6)))./amp_factor_TC));
d_TC_V = 1/((pre_d_TC_V-100)/(0-100));

f1 = figure(); hold on;
plot(TC_SR_data(:,1), TC_SR_data(:,2), 'blue o');
plot(TC_SR_fit, 'red');
errorbar(SRdataPoint/10,TC_SR_data(SRdataPoint,2),-d_SR_V./2,d_SR_V./2,'bs',...
'CapSize',20,'HandleVisibility','off')
title("Thermocouple (Al Ball Mass) Transient Response");
xlabel("Time (s)");
ylabel("ln(Theta)");
legend("Thermocouple Data","y = -0.1626x + 0.8623");
hold off;

f2 = figure(); hold on;
plot(TC_TC_data(:,1), TC_TC_data(:,2), 'blue o');
plot(TC_TC_fit, 'red');
axis([0 11 -20 1]);
errorbar(TCdataPoint/10,TC_TC_data(TCdataPoint,2),-d_TC_V./2,d_TC_V./2,'bs',...
'CapSize',20,'HandleVisibility','off')
title("Thermocouple (Regular) Transient Response");
xlabel("Time (s)");
ylabel("ln(Theta)");
legend("Thermocouple Data","y = -9.807x + 13.39");
hold off;
```

10 Appendix C: MATLAB Data Processing Script for Heat Transfer Coefficient and Fluid Velocity Estimation

```
%% Estimate fluid velocity from transient forced convection data
%Last edit by VB, 10/23

clear; clc; close all;
tau = [937.21; 201.52; 31.54; 9.38]; %Time constants (s)
dtau = [13.56; 1.18; 0.48; 0.26]; %Uncertainty of time constants (s)
d = (50.67)./1000; %Diameter of sphere [m]
r = d./2; %Radius of sphere [m]
rho = 2710; %Density of aluminum [kg/m^3]
rho1 = 1.225; %Density of air [kg/m^3]
rho2 = 997; %Density of water [kg/m^3]
k1 = 31.62./1000; %Thermal conductivity of air [W/mK]
k2 = 0.677; %Thermal conductivity of water [W/mK]
dd = 0.000005; %Uncertainty of diameter [m]
dr = dd./2; %Uncertainty of radius [m]
V = (4./3).*pi.*(r.^3); %Volume of sphere [m^3]
dV = 4.*pi.*(r.^2).*dr; %Uncertainty of volume [m^3]
m = rho.*V; %Sphere mass [kg]
dm = rho.*dV; %Uncertainty of mass [kg]
A = 4.*pi.*(r.^2); %Sphere surface area [m^2]
dA = 8.*pi.*r.*dr; %Uncertainty of surface area [m^2]
cp = 9000; %Specific heat [J/kg K]
h = (m.*cp)./(A.*tau); %Heat transfer coefficient [W/m^2k]
%Uncertainty of Heat transfer coefficient [W/m^2k]
dh = sqrt( (((cp)./(A.*tau)).*dm).^2 + (((m.*cp)./((A.^2).*tau)).*dA)...
    .^2 + (((m.*cp)./(A.*(tau.^2))).*dtau).^2 );
Nu1 = (h.*d)./(k1); %Nusselt number and uncertainty
dNu1 = sqrt( ((d.*dh)./(k1)).^2 + ((h.*dd)./(k1)).^2 );
Nu2 = (h.*d)./(k2); %Nusselt number and uncertainty
dNu2 = sqrt( ((d.*dh)./(k2)).^2 + ((h.*dd)./(k2)).^2 );
mu1 = 1.81.*(10.^-5); %Air fluid properties
pr1 = 0.701;
mu2 = 8.90.*(10.^-4); %Water fluid properties
pr2 = 1.76;
%Reynolds number and uncertainty
Re1 = ((Nu1(2,1)-2)./0.6).^2./(pr1.^(2./3));
dRe1 = dNu1(2,1).*(1./0.6).*(1./(pr1.^(2/3))).*2.*((Nu1(2,1)-2)./0.6);
u1 = (Re1.*mu1)./(rho1.*d); %Velocity of air [m/s]
du1 = sqrt( ( (mu1.*dRe1)./(rho1.*d) ).^2 + ...
    ( (Re1.*mu1.*dd)./(rho1.*(d.^2)) ).^2  );
Re2 = ((Nu2(4,1)-2)./0.6).^2./(pr2.^(2./3));
```

```
dRe2 = dNu2(4,1).*(1./0.6).*(1./(pr2.^(2/3))).*2.*((Nu2(4,1)-2)./0.6);
u2 = (Re2.*mu2)./(rho2.*d); %Velocity of water [m/s]
du2 = sqrt( ( (mu2.*dRe2)./(rho2.*d) ).^2 + ...
    ( (Re2.*mu2.*dd)./(rho2.*(d.^2) )).^2  );
```